Polymorph Nickel Titanate Nanofibers as Bifunctional Electrocatalyst Towards Hydrogen and Oxygen Evolution Reactions

(Electronic Supplementary Information)

B. Sachin Kumar,[1] Kartick Tarafder,[2] Akshatha R. Shetty,[3] A. Chitharanjan Hegde,[3] Visweswara C. Gudla,[4] Rajan Ambat,[4] Sreeram K. Kalpathy,[5] S. Anandhan,[1*]

S1. SAN/precursor salt interaction

Figure S1 depicts the schematic of the Ni^{2+} ions and Ti^{4+} complex,[1] interacting with the polar group of styrene-acrylonitrile copolymer (SAN), i.e. styrene ring and nitrile function groups of SAN.

S2. FESEM-EDS analysis of NTO nanofibers

FESEM images were used to measure the average fibre diameter (AFD) and standard deviation (SD) of nickel titanate (NTO) nanofibers using Image J software as shown in Figure S2. The mosaic structured nanoparticles in NTO nanofibers obtained at 773 K transforms to bamboo like structure NTO nanofibers with increasing pyrolysis soaking temperature to 1173 K. EDS spectra was acquired for the selected area on the NTO nanofiber. The weight and atomic percentage of each element is shown in Figure S2.

S3. Band struture of INTO and SNTO

The band structure of ilmenite NTO (INTO) and spinel NTO (SNTO) estimated from first-principles density functional theory (DFT) analysis are shown in Figure S3.

S4. XPS analysis of NTO nanofibers

Figure S4a is the XPS survey spectra of NTO nanofibers obtained at different pyrolysis soaking temperatures. Figure S5a-c are the high-resolution XPS spectra recorded for O, Ni, and Ti elements. The presence of both INTO and SNTO is confirmed in all samples of the NTO nanofibers.

S5. Hydrogen gas discharge

The increase in the volume of H_2 liberated and collected with increase in negative current is shown in Figure S5 for NTO/GE obtained from pyrolysis soaking temperature of 773 K. The quantity of H_2 evolved increases up to -300 mA and reaches saturation. Hence, this -300 mA current can be used for rest of the electrochemical studies, as H_2 discharge is maximum here.

S6. Oxygen gas discharge

The increase in the volume of O_2 liberated and collected with increase in positive current is shown in Figure S6 for NTO/GE obtained from pyrolysis soaking temperature of 1173 K. The quantity of O_2 evolved increases up to +300 mA and reaches saturation. Hence, this +300 mA current can be used for rest of the electrochemical studies, as O_2 discharge is maximum here.

S7. State-of-the-art commercially available materials

Figure S7a and S7b shows the result of the CV analysis and Tafel plot of the state-of-the-art commercial Pt/C/GE electrode for HER, respectively. The onset potential and cathodic Tafel slope (β_c) of Pt/C/GE are -0.935 V vs. SCE and 117.4 $mV \cdot dec^{-1}$, correspondingly (Figure S7b). Further, the result of the CV analysis of the state-of-the-art commercial RuO_2/GE electrode for OER are shown in Figure S7c and S7d. The onset potential and anodic Tafel slope (β_a) of RuO_2/GE are 0.417 V vs. SCE and 68.4 $mV \cdot dec^{-1}$, respectively.

References

1 B. S. Kumar, A. M. Shanmugharaj, S. K. Kalpathy and S. Anandhan, Some new observations on the structural and phase evolution of nickel titanate nanofibers, *Ceram. Int.*, 2017, **43**, 6845–6857.

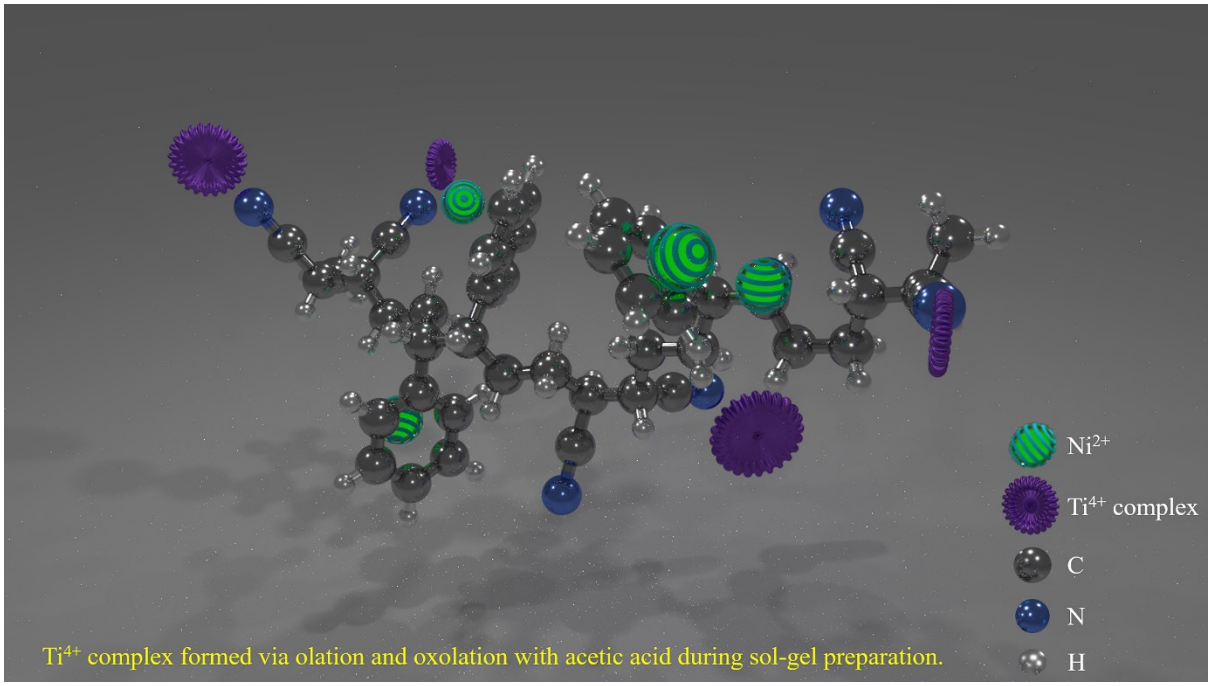

Figure S1: Schematic depicting the SAN/precursors interaction.

Electron Image (inset: EDX spectrum)	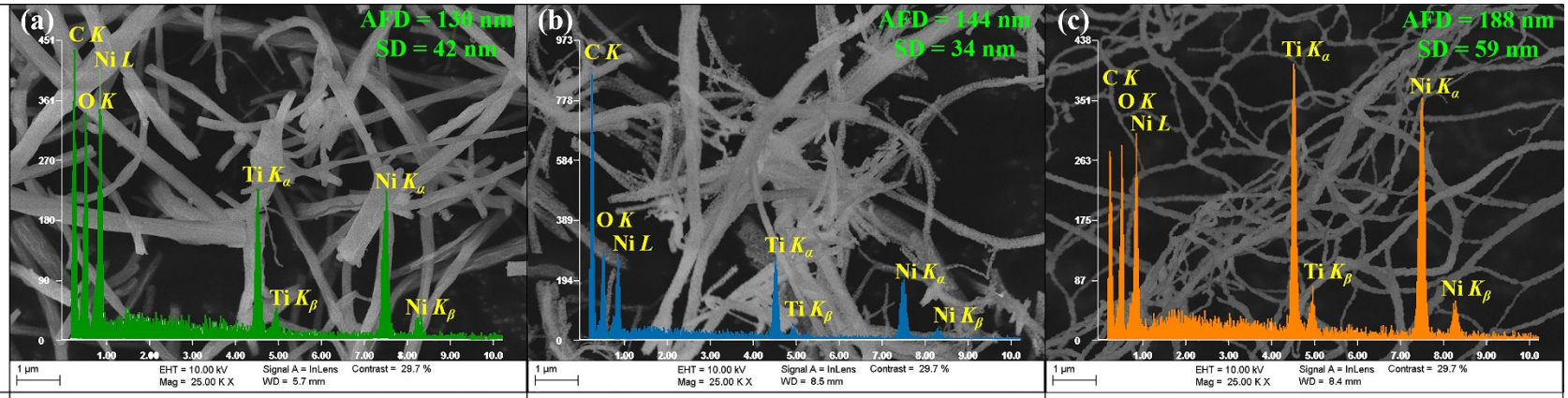						
Pyrolysis temperature (K)	**773**		**973**		**1173**	
	Weight %	**Atomic %**	**Weight %**	**Atomic %**	**Weight %**	**Atomic %**
C *K*	39.57	67.51	53.14	78.62	31.24	57.08
O *K*	16.66	21.34	12.66	14.06	15.84	21.73
Ti *K*	20.64	3.08	17.49	2.26	14.21	6.61
Ni *K*	23.13	8.07	16.71	5.06	38.71	14.58

Figure S2: FESEM micrographs depicting AFD±SD of NTO nanofibers obtained at different pyrolysis temperatures. Weight and atomic percentage of each elements present in NTO nanofibers recorded by EDS analysis.

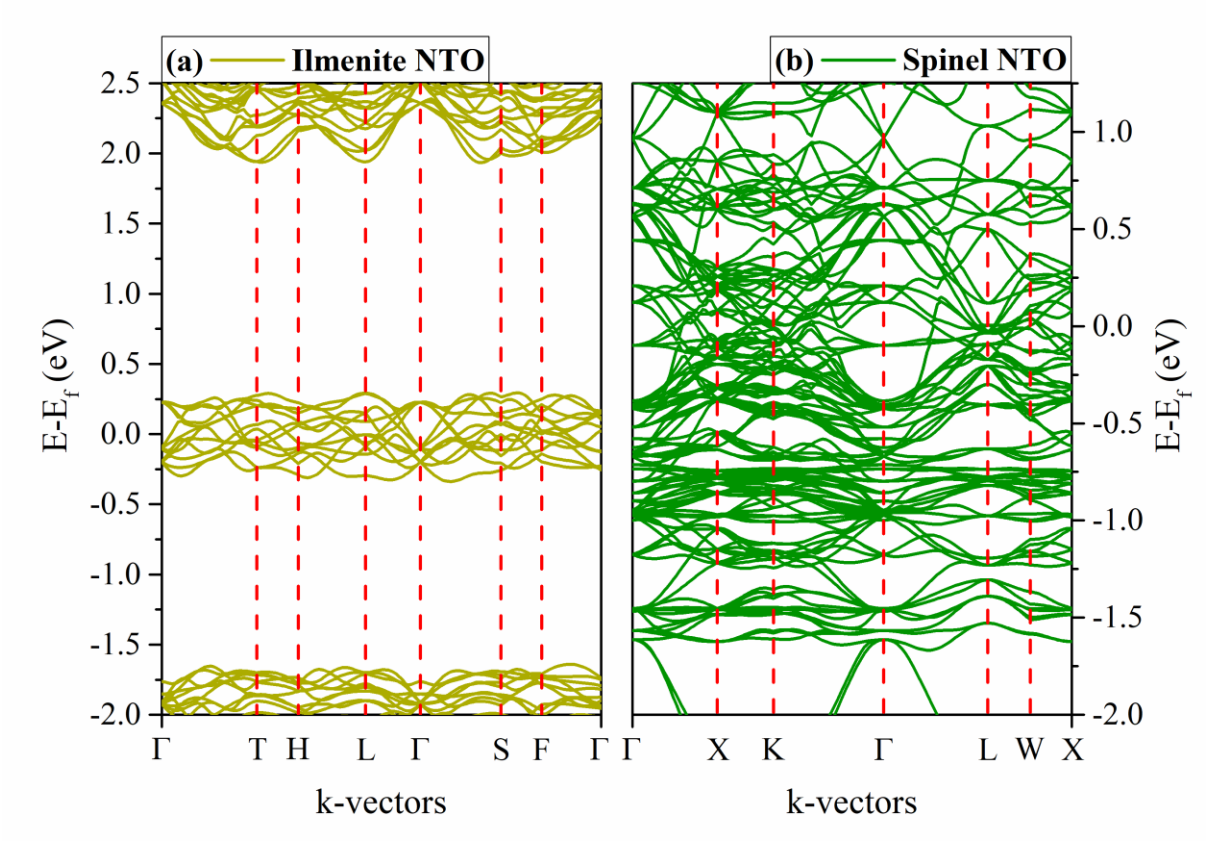

Figure S3: Comparison of band structure of (a) INTO and (b) SNTO acquired from DFT analysis.

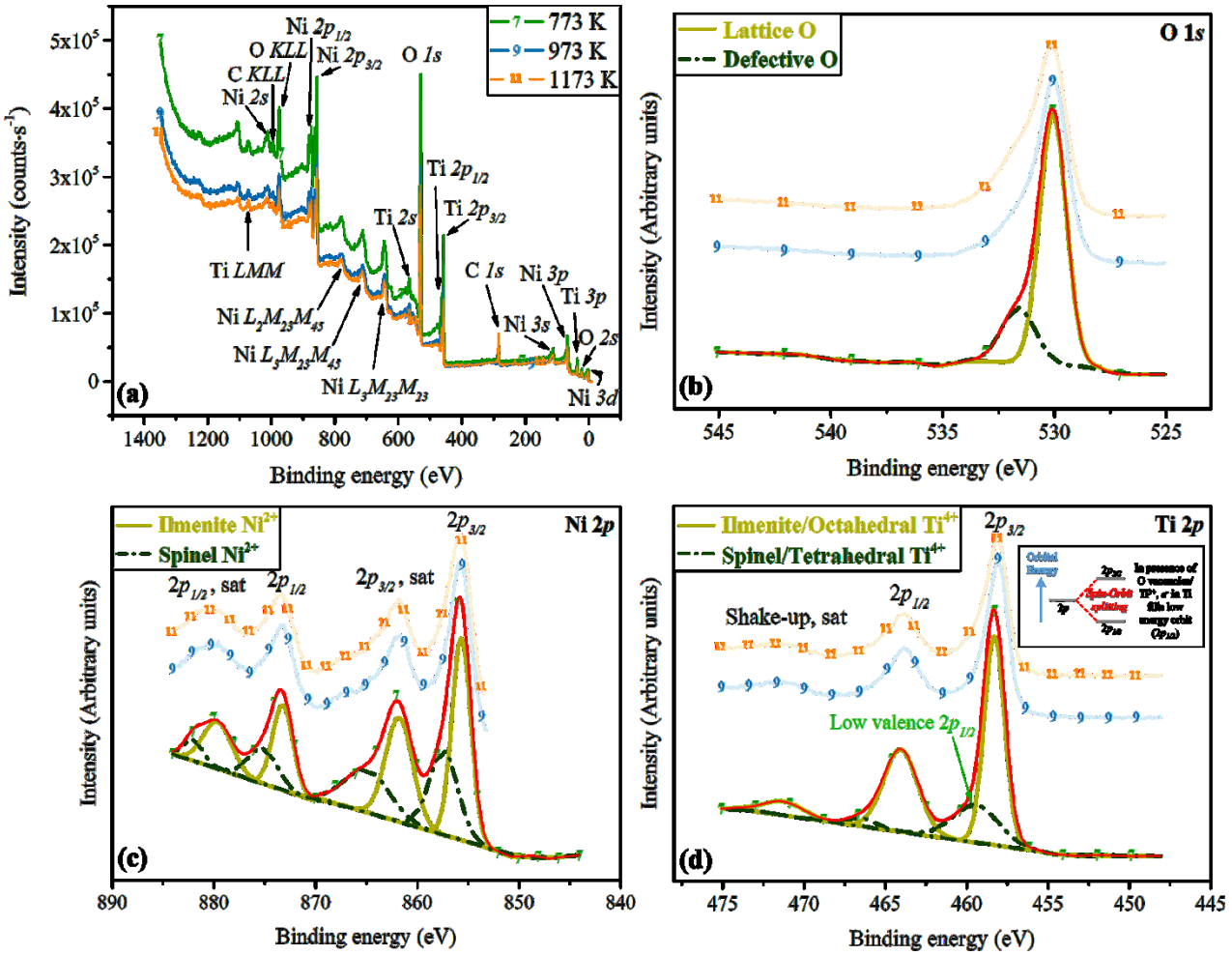

Figure S4: XPS of NTO nanofibers obtained at different pyrolysis soaking temperatures. (a) survey spectra, (b) high-resolution spectra for O *1s*, (c) high-resolution spectra for Ni *2p*, and (d) high-resolution spectra for Ti *2p* (inset figure: spin-orbit splitting for Ti^{3+} ion). The deconvoluted peaks in each individual graph are representative and similar deconvoluted peaks exists in all the three high-resolution spectra of corresponding graph.

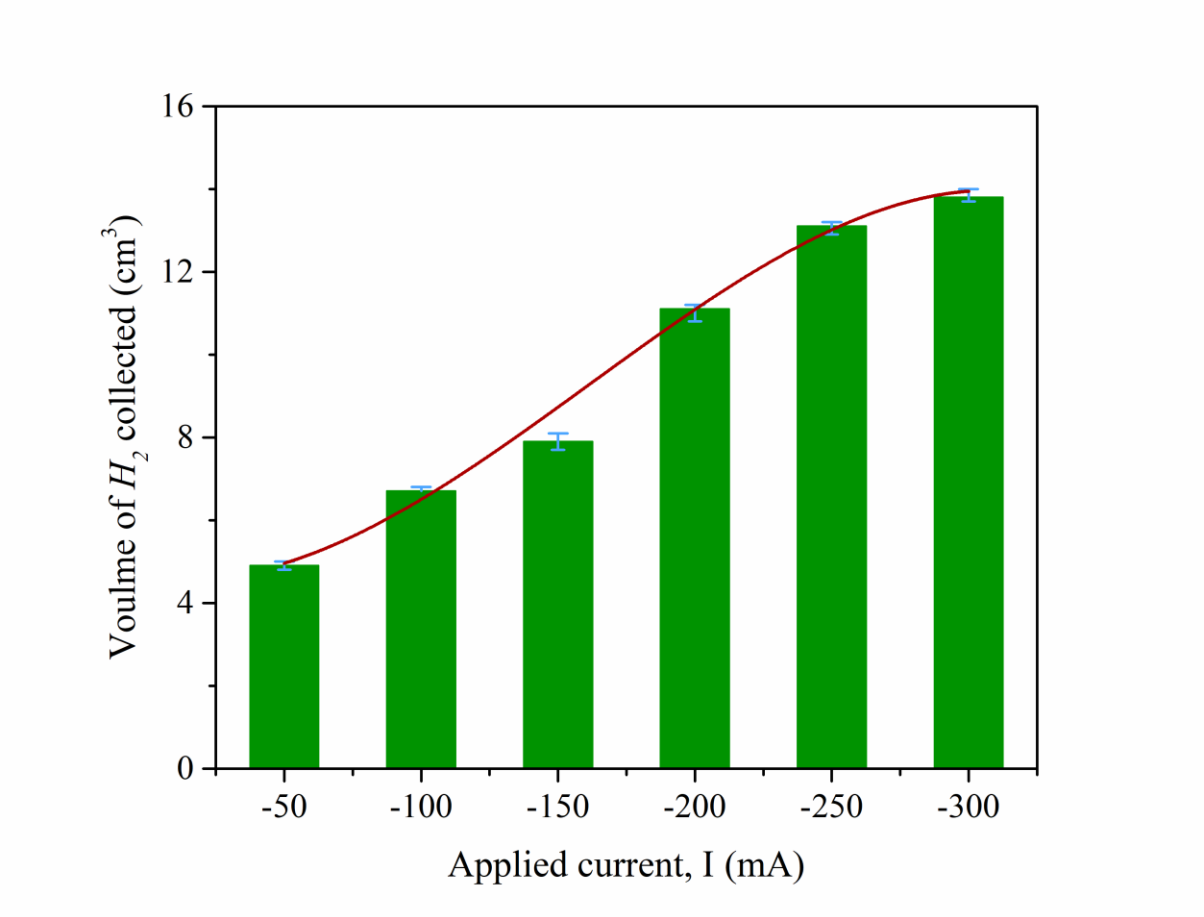

Figure S5: Quantity of H_2 liberated with respect to current for NTO/GE developed at pyrolysis soaking temperature of 773 K.

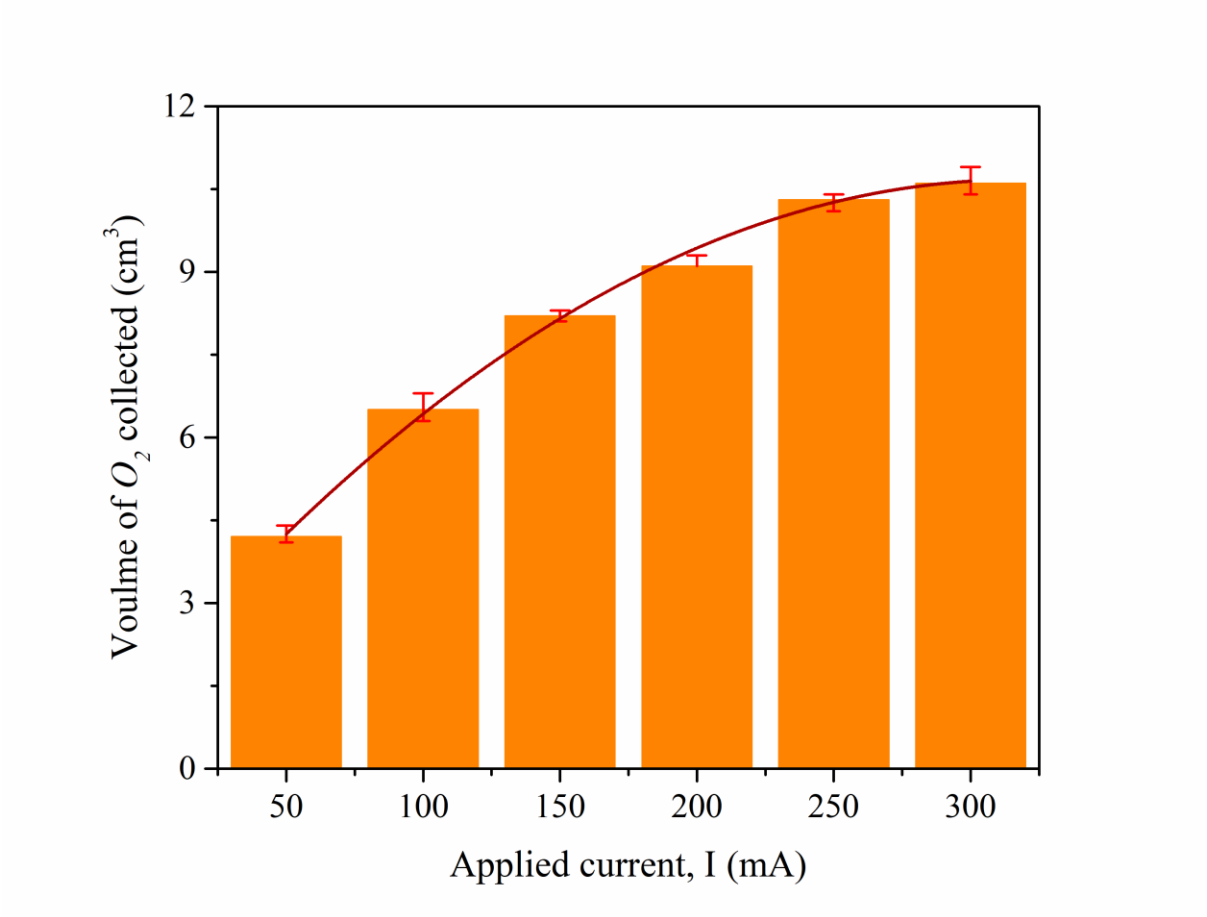

Figure S6: Quantity of O_2 liberated with respect to current for NTO/GE developed at pyrolysis soaking temperature of 1173 K.

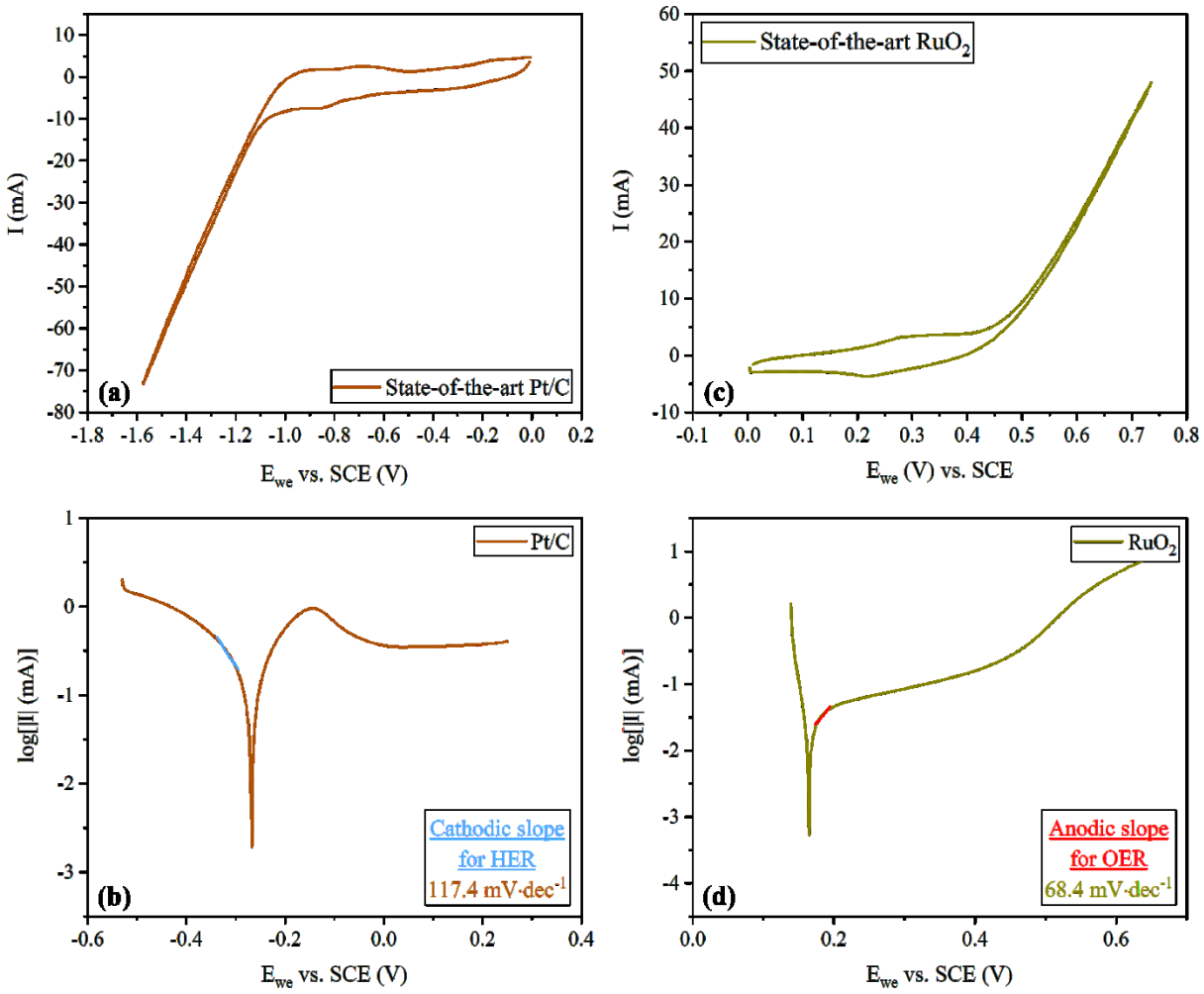

Figure S7: CV analysis and Tafel plot of the state-of-the-art commercial Pt/C/GE electrode for HER (a, b) and RuO_2/GE for OER (b, d).